Journal of Luminescence 206 (2019) 565–570

Contents lists available at ScienceDirect

Journal of Luminescence

journal homepage: www.elsevier.com/locate/jlumin

# One-step hot injection synthesis of gradient alloy $Cd_xZn_{1-x}S_ySe_{1-y}$ quantum dots with large-span self-regulating ability

Hanan Osman[a,b,1], Wen Li[a,1], Xueqiao Zhang[c], Fengjun Chun[a], Wen Deng[a], Marwa Moatasim[a], Xiaotong Zheng[a], Weili Deng[a], Haitao Zhang[a], Weiqing Yang[a,*]

[a] Key Laboratory of Advanced Technologies of Materials (Ministry of Education), School of Materials Science and Engineering, Southwest Jiaotong University, Chengdu 610031, China
[b] Electronics and Computational Physics Department, Faculty of Science and Technology, AL Neelain University, Khartoum 12702, Sudan
[c] University of Washington, 1410 NE Campus Parkway, Seattle, WA 98195, USA

ARTICLE INFO

*Keywords:*
Quantum dots
Alloyed $Cd_xZn_{1-x}S_ySe_{1-y}$
Luminescent materials
Composition tunability
One-step hot injection synthesis

ABSTRACT

CdSe-derived quantum dots (QDs) materials are highly luminescent and have been promisingly implementing a wide range of applications. However, CdSe-derived QDs with controllable emission wavelength and composition always require a highly complicated synthetic process, which badly hinders its mass production. Here, we present a simple one-step hot injection method to synthesize the versatile $Cd_xZn_{1-x}S_ySe_{1-y}$ (x = 0.12, 0.17, 0.23, 0.33, y = 0, 0.64, 1) QDs with controllable composition and large-span emission wavelengths. Only by varying the molar ratios of Cd to Zn and Se to S, the emission wavelength span of the as-obtained gradient alloyed $Cd_xZn_{1-x}S_ySe_{1-y}$ QDs is widely closed to 200 nm (445–643 nm), and the narrow full width at half-maximum surprisingly emerges down to 14 nm, evidently revealing that excellent self-regulating ability and superior monochromaticity. Using these different coloured QDs, we fabricate the typical red, yellow and blue light emitting diode (LED) lamps integrated with the ultraviolet chip (365 nm), showing steady and bright emission. The above results afford an efficient method to control the optical properties of QDs and ensure their processibility for further purposes in variable optoelectronics.

## 1. Introduction

Colloidal semiconductor nanocrystals with shape-, size-, and composition-dependent properties have been widely sought for broad applications, in the fields of solar cells, light-emitting diodes (LED) and biological labels [1–6]. Over the past decade, II-IV semiconductor nanocrystal, CdSe quantum dot (QD), which has been known to localize due to its narrow size distribution and distinct quantum confinement effect, joined the family of semiconductor QDs used for light-emitting diodes, as a very promising candidate [7,8]. However, considering the increased surface to volume ratio of QDs, the destruction by defects and surface-trap states are still significant threatens to the luminescence efficiency and stability of CdSe QDs [9]. Due to the much stronger damage, a surface-passivation strategy is needed to mitigate this problem by enclosing CdSe QDs with suitable organic or inorganic shell [10]. Although this method can reduce the nonradiative recombination centers, the organic capping materials may be more prone to chemical degradation or photooxidation, and the lattice mismatch between core and inorganic shell interface will form defects like interfacial misfit dislocation, which dramatically decrease the quantum efficiency of QDs [2,11,12]. Therefore, an alternative strategy for producing alloyed QDs is explored to synthesize composition-dependent and luminescent tunable QDs without sacrificing the chemical stability.

An appealing aspect of alloyed semiconductor QDs is that tailored optical properties can be obtained only by controlling the proportion of different reaction precursors. Zhong and co-workers reported high-quality ternary $Zn_xCd_{1-x}Se$ alloy nanocrystals with emission efficiency ranging from 70% to 85%; it is of great importance to find temperatures (alloying point) for the incorporation of Zn and Se into pre-prepared CdSe nanocrystals [13]. Successively, this research group also synthesized ternary $Zn_xCd_{1-x}S$ alloy nanocrystals with extremely narrow emission spectral widths at high temperature by adjusting the Zn/Cd molar ratios of the reaction precursors via one-pot process [14]. Subhendu and co-workers demonstrated gradated alloyed CdZnSe QDs with quasi core/shell structure, tunable emission wavelengths at the range 500–650 nm were achieved by extending the alloying time for the

* Corresponding Author.
*E-mail address:* wqyang@swjtu.edu.cn (W. Yang).
[1] These authors contributed equally to this work.

https://doi.org/10.1016/j.jlumin.2018.10.089
Received 27 April 2018; Received in revised form 17 October 2018; Accepted 19 October 2018
Available online 22 October 2018
0022-2313/ 

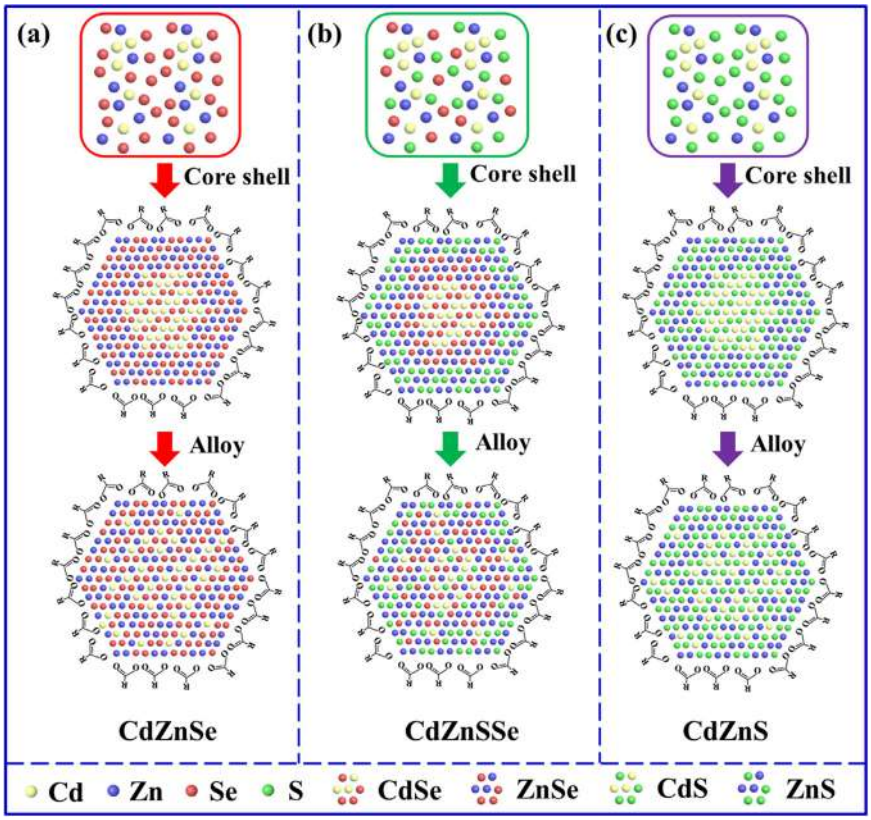


**Fig. 1.** Synthetic scheme of alloyed $Cd_xZn_{1-x}S_ySe_{1-y}$ QDs ($Cd_xZn_{1-x}S_ySe_{1-y}$ QDs changed from core-shell structure to alloy compounds). (a) only Se, $Cd_xZn_{1-x}Se$; (b) mixed S and Se, $Cd_xZn_{1-x}S_ySe_{1-y}$; (c) only S, $Cd_xZn_{1-x}S$.

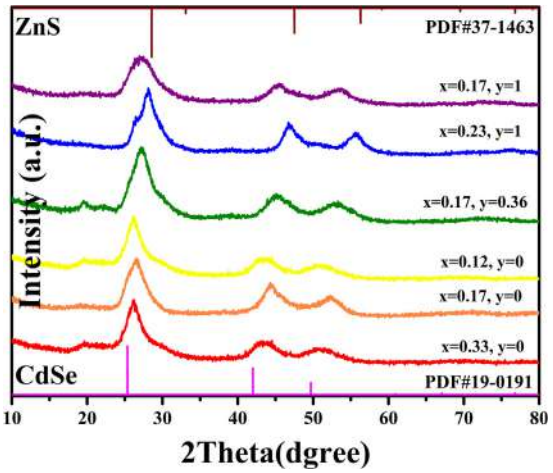


**Fig. 2.** XRD patterns for composition tunable $Cd_xZn_{1-x}S_ySe_{1-y}$ QDs (x = 0.12, 0.17, 0.23, 0.33, y = 0, 0.64, 1).

formation of gradated chemical composition [15]. In addition, homogeneous quaternary ZnCdSSe QDs were synthesized with tunable emission wavelength (516–550 nm) by using a one-pot synthesis method with the assistance of increasing the reaction time [16]. Despite the works mentioned above showed a color-tunable emission of the ternary and quaternary alloyed QDs, the simple and reproducible one-step process of synthesizing alloyed QDs with controllable composition and large-span emission wavelengths remain a challenge to date [17–23].

In this work, we demonstrate a more facile and highly reproducible one-step hot injection synthesis (OHIS) technology, which enables controllable phase component and large-span luminescence wavelength regulation of high-quality $Cd_xZn_{1-x}S_ySe_{1-y}$ QDs. The surprisingly large span (about 200 nm) from red to purple emitting (643–445 nm) QDs with nearly monodispersed particle sizes can be obtained only by varying the Cd to Zn and S to Se molar ratios, much wider than that (about 34 nm) of the other one-step synthesis. The effects of the atomic ratios on the phase component and optical properties of series QDs were investigated in detail. Furthermore, the typical red, yellow and blue LED prototypes are further fabricated by employing the as-prepared $Cd_xZn_{1-x}S_ySe_{1-y}$ QDs as color conversion materials. This simple OHIS method provides a vast opportunity to realize the large-span luminescent wavelength and large-scale production of the high-quality QDs.

## 2. Experimental section

### 2.1. Preparation of $Cd_xZn_{1-x}S_ySe_{1-y}$ QDs

Cadmium oxide (CdO, purity 99.99%), zinc acetate ($Zn(Ac)_2$, purity 99.9%), sulfur powder (S, purity 99.99%), selenium powder (Se, purity 99.99%), octadecene (ODE, purity 90%), trioctylphosphine (TOP, purity 90%) and oleic acid (OA, purity 99.99%) were purchased from Sigma-Aldrich. All reagents were used as received without further experimental purification.

The colloidal alloyed $Cd_xZn_{1-x}S_ySe_{1-y}$ QDs were synthesized as following. For a typical synthesis of green QDs (x = 0.17, y = 0.36), the TOPSSe solution was prepared at first by mixing Se powder (2.7 mmol), S powder (1.5 mmol) and TOP (2.5 mL) into 5 mL vial and stirring to obtain a clear solution at room temperature. Next, the Cd-$(oleate)_2$ and Zn-$(oleate)_2$ solution was prepared by adding CdO (0.98 mmol), Zn $(Ac)_2$ (3.22 mmol), OA (6 mL) and ODE (15 mL) into 100 mL three-neck round bottom flask. The solution was drying under vacuum at 130 °C for 30 min to remove the oxygen and water. Then the solution was heated to 300 °C under a high-purity $N_2$ atmosphere. At this elevated temperature, as-prepared TOPSSe solution (2.5 mL) was swiftly injected

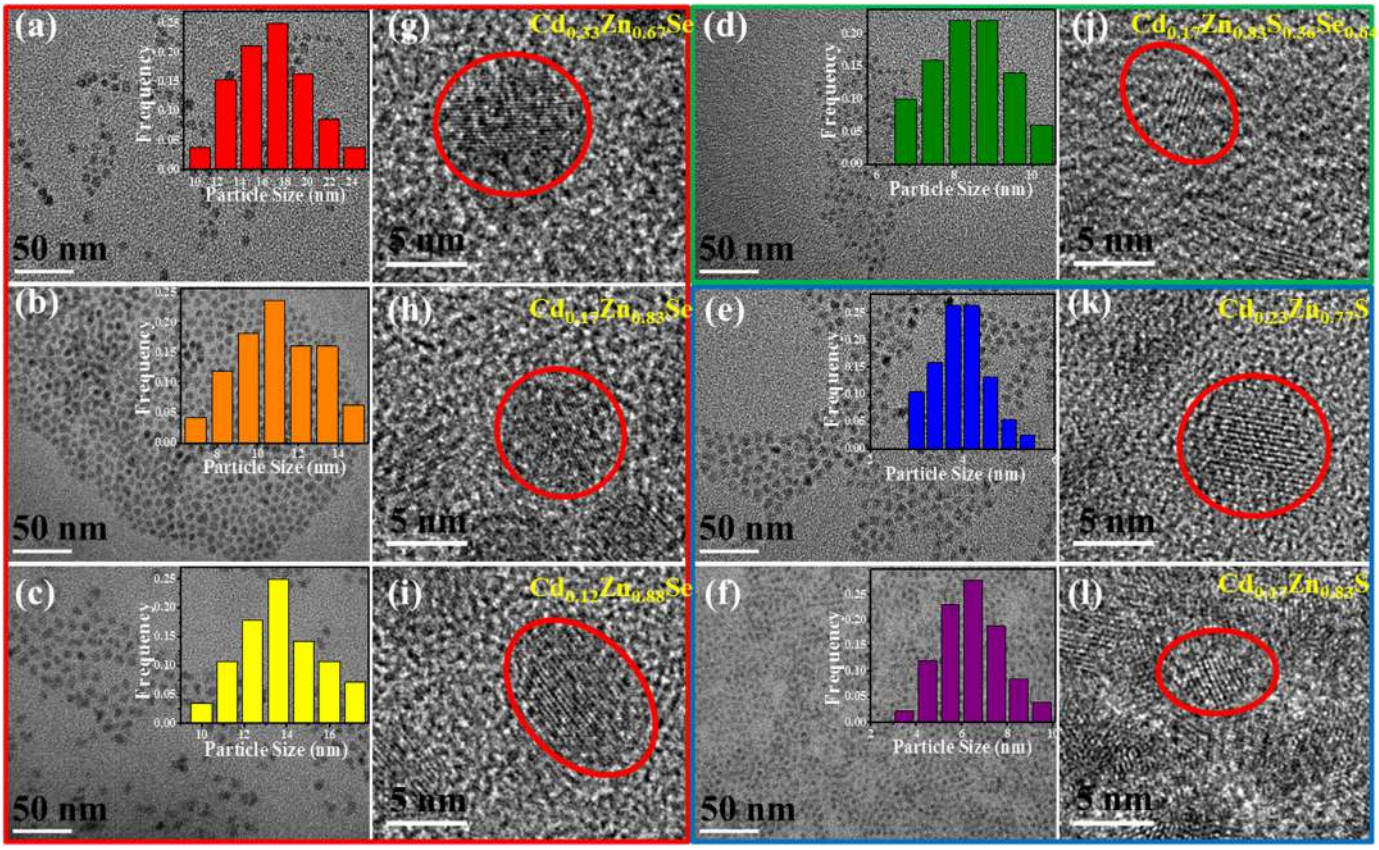


**Fig. 3.** The micromorphology of as-prepared QDs. (a-f) TEM and (g-l) HRTEM characterization for $Cd_xZn_{1-x}S_ySe_{1-y}$ QDs with different composition. The insets are size distribution histograms of $Cd_xZn_{1-x}S_ySe_{1-y}$ QDs.

into the Cd-(oleate)$_2$ and Zn-(oleate)$_2$ solution. The reaction temperature was maintained at 300 °C for 10 min then cooled to room temperature naturally, and strong green emission was observed. Finally, the product was purified several times by repeating the precipitation/redispersion processes using methanol and toluene; the acquired precipitate was redispersed in toluene or collected as powder for characterization.

Other $Cd_xZn_{1-x}S_ySe_{1-y}$ QDs with different colors were fabricated with the variable values of x and y while maintaining the total powder mixture of CdO and Zn(Ac)$_2$ is 4.2 mmol, as well as the total 4.2 mmol of Se and S powder. Other parameters such as the amount of solvent, reaction temperature and reaction time remain the same. When the addition amount of Se powder is 4.2 mmol (y = 0), three types of $Cd_xZn_{1-x}Se$ QDs were synthesized under similar condition except different addition amount of CdO and Zn(Ac)$_2$. As x values were 0.33, 0.17 and 0.12, the amounts of CdO were 1.4 mmol, 0.7 mmol and 0.5 mmol, corresponding amounts of Zn(Ac)$_2$ were 2.8 mmol, 3.5 mmol and 3.7 mmol, red, orange and yellow $Cd_xZn_{1-x}Se$ QDs can be obtained with their corresponding CdO:Zn(Ac)$_2$ M ratio of 1:2, 1:5 and 1:7.4. When the addition amount of S powder is 4.2 mmol (y = 1), $Cd_xZn_{1-x}S$ QDs with blue (x = 0.23) and purple (x = 0.17) emission were synthesized, and the amounts of CdO and Zn(Ac)$_2$ were (0.97 mmol, 0.7 mmol) and (3.23 mmol, 3.5 mmol), and their corresponding CdO:Zn(Ac)$_2$ molar ratios are 1:3.3 and 1:5.

### 2.2. Construction of QDs-LED lamps

As the first step, $Cd_xZn_{1-x}S_ySe_{1-y}$ QDs powder (15 wt%) were dispersed in a small volume of silicone A (17 wt%) stirring for 2 h to ensure fine dispersion of the individual QDs. The mixture was then added to a large volume of silicone B (68 wt%) which acted as a curing agent stirring for 1 h to facilitate QDs dispersion. Then the mixture needed vacuum defoamation for 1 h. A small drop of the homogeneous QDs/silicone composite was casted onto the surface of an ultraviolet LED chip (centered at 365 nm) using a toothpick. Subsequently, the lamp was dried at 60 °C for 40 min to mix the composite thoroughly. Finally, the LED lamp was thermal-treated at 135 °C for 110 °C to cure the QDs/silicone composite and improve the anti-fading effect. When the temperature was cooled to room temperature, the monochromatic LED lamp was obtained.

### 2.3. Characterization

Steady-state photoluminescence (PL) spectra were carried out using FLS 980 (Edinburgh Instruments). Powder X-ray diffraction (XRD) data was recorded using a Bruker D8 Advance X-ray diffractometer using Cu Kα radiation (1.54 Å). Transmission electron microscopy (TEM) studies were carried out using a JEOL JEM 2100 F field emission transmission electron microscope at 200 kV. Steady-state absorption spectra were recorded on a Shimadzu UV-2600 spectrophotometer. Photoluminescence quantum yield (PLQY) was measured with an absolute method using FLS980 and the integrating sphere.

## 3. Results and discussions

The proposed reaction mechanism for three typical cases is schematically drawn in Fig. 1, only Se, only S and mixed S-Se chalcogenides. Because the reactivity of Zn precursor is much lower than that of Cd precursor, Zn-(oleate)$_2$ is more thermostable than Cd-(oleate)$_2$. Similarly, the reactivity of Se is more vivid than that of S, which will determine the phase composition of the intermediate product [2,24,25]. Furthermore, the standard Gibbs free energy change for the formation of CdSe, ZnSe, CdS and ZnS are gradually increasing, which promising that CdSe would be formed by preferential reactivity once again [16].

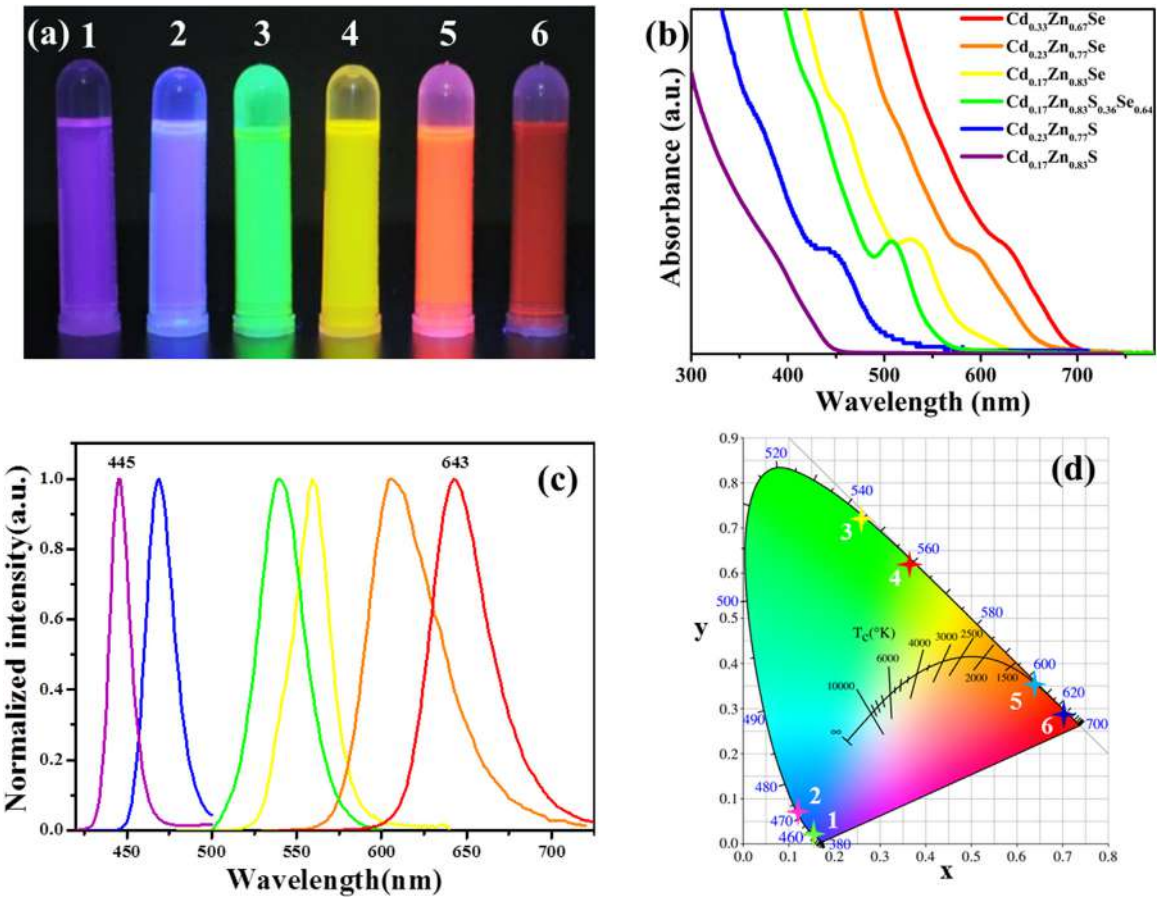


**Fig. 4.** The optical properties of as-prepared QDs. (a) The digital photographs of $Cd_xZn_{1-x}S_ySe_{1-y}$ QDs under the irradiation of a UV lamp; (b) Absorption spectra for $Cd_xZn_{1-x}S_ySe_{1-y}$ QDs; (c) PL spectra of composition tunable $Cd_xZn_{1-x}S_ySe_{1-y}$ QDs; (d) The color coordinates of $Cd_xZn_{1-x}S_ySe_{1-y}$ QDs on CIE1931 chromaticity diagram.

**Table 1**
Emission peaks, full width at half-maximum (FWHM) and quantum yields of the as-prepared $Cd_xZn_{1-x}S_ySe_{1-y}$ QDs.

| Sample | Emission peak (nm) | FWHM (nm) | QY (%) |
|---|---|---|---|
| $Cd_{0.33}Zn_{0.67}Se$ | 643 | 41 | 64 |
| $Cd_{0.23}Zn_{0.77}Se$ | 606 | 45 | 66.8 |
| $Cd_{0.17}Zn_{0.83}Se$ | 559 | 28 | 60 |
| $Cd_{0.17}Zn_{0.83}S_{0.36}Se_{0.64}$ | 539 | 30 | 89 |
| $Cd_{0.23}Zn_{0.77}S$ | 468 | 19 | 56 |
| $Cd_{0.17}Zn_{0.83}S$ | 445 | 14 | 38 |

For the S-Se mixed chalcogenide sample (Fig. 1b), CdSe core will be formed at the early stage; if Se precursor is not consumed at all when Cd has been depleted, the ZnSe shell will be formed around the CdSe core. As the Se precursor runs out, another ZnS shell will be wrapped up. As a result, a CdSe/ZnSe/ZnS core-shell structure will be formed firstly. However, ion exchange occurs within the core-shell structure as the reaction time prolongs at high temperature. In the alloying process, ligands can form a molecular layer on the surface of QDs and prevent aggregation. As the cations ($Cd^{2+}$, $Zn^{2+}$) diffuse much more comfortable than the anions ($S^{2-}$, $Se^{2-}$), the CdSe/ZnSe/ZnS core-shell can be converted into alloyed CdZnSSe QDs [26,27]. So as the only S and Se chalcogenide samples, the alloyed CdZnS and CdZnSe QDs are achieved as illustrated in Fig. 1a and c, which demonstrates a simple route to prepare composition tunable CdZnSe QDs.

The XRD patterns of as-synthesized composition tunable $Cd_xZn_{1-x}S_ySe_{1-y}$ QDs are presented in Fig. 2 and compared with patterns from standard JCPDS card of CdSe (NO.19–0191) and ZnS (NO.37–1463). The results show that the diffraction peaks of $Cd_xZn_{1-x}S_ySe_{1-y}$ QDs gradually shift to larger angles from the bottom to the top sample, and all the diffraction peaks locate between the standard bulk CdSe and ZnS. Comparing $Cd_{0.17}Zn_{0.83}Se$, $Cd_{0.17}Zn_{0.83}S_{0.36}Se_{0.64}$ and $Cd_{0.17}Zn_{0.83}S$ QDs, the larger Se atoms (1.98 Å) were substituted by smaller S atoms (1.84 Å), leading to the shift of main diffraction peaks toward higher angles [28]. The result is indicative of the decrease in lattice parameter due to the smaller ionic radius of Zn relative to that of Cd, which is consistent with Vegard's law. For $Cd_xZn_{1-x}Se$ QDs, the increase of Zn constituent incorporated into alloyed QDs contributes to shift of characteristic diffraction peak as x decreases from 0.33 to 0.12. No other characteristic peaks belonged to CdS(e) and ZnS(e) could be identified in XRD patterns, indicating a compositional homogeneity phase of $Cd_xZn_{1-x}S_ySe_{1-y}$ rather than a mixture of CdS(e) and ZnS(e). Also, it is worth noting that the uniformly continuous peak shifting further proves that the product synthesized by the OHIS method is an alloyed QDs. Furthermore,the apparent peak broadening was exhibited owing to the small crystalline size of the prepared QDs; this deduction can be verified in the following TEM test.

For the deep-going insight into as-prepared QDs, Fig. 3 depicts a series of TEM and HRTM images of the composition dependent alloyed $Cd_xZn_{1-x}S_ySe_{1-y}$ QDs. All the nearly monodispersed QDs reveal uniform spherical structure with well-resolved lattice fringes, clearly confirming the high crystallinity of the alloyed QDs [5]. There is no evidence of the presence of apparent core-shell interface in all QDs, and lattice fringes penetrate the entire QD, suggesting epitaxial growth for the alloyed QDs [29,30]. The size of gradient alloyed QDs are changed by the atomic substitution between Cd and Zn or S and Se, and particle size distribution histograms of QDs collected at different composition are shown in the inset of Fig. 3. In view of the different precursor reactivity, the size of the alloyed QDs under the same reaction condition is

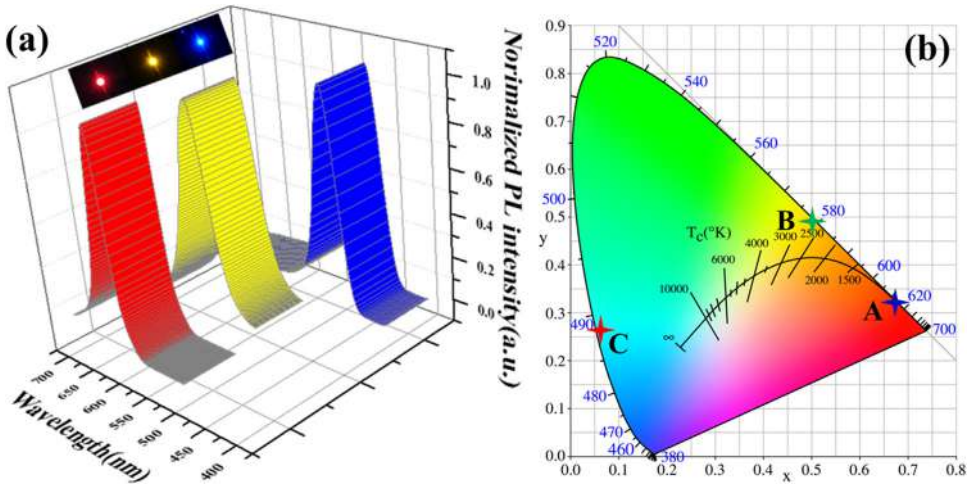


**Fig. 5.** The optical properties of three LED lamps. (a) The spectra characteristics of three typical as-prepared QDs based LED lamps operated at 3 V. The inset is the photograph of LED lamps with different emission color under a dark condition. (b) The color coordinates of three LED samples on the CIE1931 chromaticity diagram.

different. For alloyed $Cd_{0.17}Zn_{0.83}S_{0.64}Se_{0.36}$ QDs, the estimated particle size is approximately 8.5 nm. Only when Se is present in alloyed QDs, with increasing Zn content, the size of the $Cd_{0.33}Zn_{0.67}Se$, $Cd_{0.17}Zn_{0.83}Se$ and $Cd_{0.12}Zn_{0.88}Se$ QDs are about 17.5, 11.0 and 13.5 nm respectively. Similarly, when only S is present, the sizes are 6 and 4 nm for alloyed $Cd_{0.23}Zn_{0.77}S$ and $Cd_{0.17}Zn_{0.83}S$ QDs, respectively, as the Zn content increases. The results obviously demonstrate that the relatively higher reactive precursor (Cd-(oleate)$_2$ and TOPSe) the larger size ($Cd_xZn_{1-x}Se$), while the lower reactivity (Zn-(oleate)$_2$ and TOPS), the smaller size ($Cd_xZn_{1-x}S$).

The luminescent properties of gradient alloyed $Cd_xZn_{1-x}S_ySe_{1-y}$ QDs were investigated and displayed in Fig. 4, demonstrating that the simple OHIS method successfully prepared composition tunable $Cd_xZn_{1-x}S_ySe_{1-y}$ QDs with wide emission wavelengths. By changing the ratios of Cd to Zn and S to Se, six typical samples were obtained which emitted six different color (red, orange, yellow, green, blue and purple) shown in Fig. 4a. The color change observed upon varying the precursor composition is quantified by PL emission (Fig. 4c) and UV−vis absorption spectra (Fig. 4b). The PL emission can be tuned to cover the visible spectral range (from 445 to 643 nm) by adjusting the composition of alloyed $Cd_xZn_{1-x}S_ySe_{1-y}$ QDs. The UV−vis absorption spectra show single absorption peaks, and the emission spectra exhibit Stokes shift with respect to their absorption spectra. The continuous shift of the absorption and PL spectra of the alloyed $Cd_xZn_{1-x}S_ySe_{1-y}$ QDs with different compositions further confirms the alloying process. For $Cd_xZn_{1-x}Se$ QDs, the emission wavelengths gradually blue-shift as the x increases from 0.12 to 0.33, clearly meaning that the more Zn incorporation will achieve the shorter emission wavelength. Similarly, compared with $Cd_xZn_{1-x}Se$ QDs, $Cd_xZn_{1-x}S$ and $Cd_xZn_{1-x}S_ySe_{1-y}$ QDs also blue shift with the increase of S content. The PL peaks demonstrate the remarkable blue shift from 643 to 445 nm upon the different Cd to Zn and S to Se ratios; this systematic change will cause the variation in the optical gap of the gradient alloyed QDs which contribute to versatile emission colors [31]. These observations clearly provide conclusive evidence for the formation of the alloyed $Cd_xZn_{1-x}S_ySe_{1-y}$ QDs, rather than intermixing the binary II-VI QDs contents, CdS(e) and ZnS(e). In Fig. 4c, there is also no corresponding PL peaks of CdS(e) and ZnS(e) QDs, which is in good agreement with the results of XRD measurements. The controllability of QDs composition via this convenient method is further confirming by regulated color coordinates shown in Fig. 4d, the varied color coordinates of six samples from purple to red QDs are (0.1572, 0.0188), (0.1231, 0.0686), (0.2628, 0.7157), (0.366, 0.6186), (0.6444, 0.3552) and (0.7104, 0.2895) respectively. Furthermore, Table 1 lists the emission of full width at half-maximum (FWHM) of the composition-dependent $Cd_xZn_{1-x}S_ySe_{1-y}$ QDs, ranging from 48 to 14 nm for six emitting samples. In order to accurately evaluate the quality of the alloyed $Cd_xZn_{1-x}S_ySe_{1-y}$ QDs, the absolute quantum yields of the as-synthesized QDs were calculated and are shown in Table 1. Moreover, the green $Cd_xZn_{1-x}S_ySe_{1-y}$ QDs containing mixed S and Se exhibit high PLQY near 89%, whereas the purple $Cd_{0.17}Zn_{0.83}S$ QDs indicate considerably low PLQY of only 38%.

Based on these as-grown QDs, we successfully constructed three typical monochromatic LED lamps using $Cd_{0.17}Zn_{0.83}Se$, $Cd_{0.12}Zn_{0.88}Se$ and $Cd_{0.23}Zn_{0.77}S$ QDs with commercially available 365 nm ultraviolet LED chips. As shown in the inset of Fig. 5a, three LED lamps show pure and bright emission at 3 V under a dark condition. The narrow emission spectra of the three LED lamps strongly confirmed the excellent monochromaticity of red, yellow and blue LED lamps in Fig. 5a. Commission International de I'Eclairage (CIE) 1931 × –y chromaticity diagram of three typical monochromatic LED lamps are presented in Fig. 5b, and the corresponding CIE chromaticity coordinates for these LED lamps were located at A (0.6775, 0.3223), B (0.5069, 0.4913) and C (0.0630, 0.2654). Moreover, the device can effectively work well even after the QDs thermal-treated at 135 °C, certainly indicating the as-prepared QDs have promising application in the optoelectronics field against the harsh environment. These high performance LEDs lamps based on as-prepared QDs unambiguously demonstrate this simple and scalable OHIS technology should be a promising method to effectively exploit the novel similar QDs for the wide applications of LEDs and next generation display techniques as well as other photoelectronics devices.

## 4. Conclusion

In summary, a simple one-step hot injection method was employed to synthesize the gradient alloy $Cd_xZn_{1-x}S_ySe_{1-y}$ QDs with enhanced luminescent self-regulating ability. The as-obtained alloyed $Cd_xZn_{1-x}S_ySe_{1-y}$ QDs surprisingly present the widely tunable emission wavelength from 445 to 643 nm, and the corresponding narrow full width at half-maximum is down to 14 nm due to excellent self-regulating ability and superior monochromaticity. The as-grown QDs were applied to successfully encapsulate the typical red, yellow and blue QDs-LED lamps with the ultraviolet chip (365 nm). These QDs-LED lamps show excellent stability and high emission performance. Therefore, we believe that the simple one-step hot injection technology will provide a promising solution to enhance the expanded emission wavelength controllability and highly luminescent performance of QDs and effectively to lower the production cost for the promotion of QDs-LED commercialization process as well as variable optoelectronics.

## Acknowledgments

This work is supported by the Scientific and Technological Projects for Distinguished Young Scholars of Sichuan Province, China (No. 2015JQ0013), the Fundamental Research Funds for the Central Universities of China (A0920502051408-10 and ZYGX2009Z0001).

## References

[1] M.A. Reed, J.N. Randall, R.J. Aggarwal, R.J. Matyi, T.M. Moore, A.E. Wetsel, Observation of discrete electronic states in a zero-dimensional semiconductor nanostructure, Phys. Rev. Lett. 60 (1988) 535–537.
[2] P. Reiss, M. Carrière, C. Lincheneau, L. Vaure, S. Tamang, Synthesis of semiconductor nanocrystals, focusing on nontoxic and earth-abundant materials, Chem. Rev. 116 (2016) 10731–10819.
[3] C.-C. Hung, S.-J. Ho, C.-W. Yeh, G.-H. Chen, J.-H. Huang, H.-S. Chen, Highly luminescent dual-color-emitting alloyed $Zn_xCd_{1-x}Se_yS_{1-y}$ quantum dots: investigation of bimodal growth and application to lighting, J. Phys. Chem. C 121 (2017) 28373–28384.
[4] S. Chatterjee, U. Maitra, A novel strategy towards designing a CdSe quantum dot–metallohydrogel composite material, Nanoscale 8 (2016) 14979–14985.
[5] Y.C. Pu, Y.J. Hsu, Multicolored $Cd_{1-x}Zn_xSe$ quantum dots with type-I core/shell structure: single-step synthesis and their use as light emitting diodes, Nanoscale 6 (2014) 3881–3888.
[6] W.W. Yu, X.G. Peng, Formation of High-quality CdS and other II-VI semiconductor nanocrystals in noncoordinating solvents: tunable reactivity of monomers, Angew. Chem. 41 (2002) 2368–2371.
[7] R.D. Rajapaksha, M.I. Ranasinghe, The shell thickness and surface passivation dependence of fluorescence decay kinetics in CdSe/ZnS core-shell and CdSe core colloidal quantum dots, J. Lumin. 3 (2016) 1600868.
[8] D. Yao, W. Xin, Z. Liu, Z. Wang, J. Feng, C. Dong, H. Zhang, Phosphine-free synthesis of metal chalcogenide quantum dots by directly dissolving chalcogen dioxides in alkylthiol as the precursor, ACS Appl. Mater. Interfaces 9 (2017) 9840–9848.
[9] I.L. Medintz, H.T. Uyeda, E.R. Goldman, H. Mattoussi, Quantum dot bioconjugates for imaging, labelling and sensing, Nat. Mater. 4 (2005) 435–446.
[10] X.M. Liu, Y. Jiang, F.M. Fu, W.M. Guo, W.Y. Huang, L.J. Li, Facile synthesis of high-quality ZnS, CdS, CdZnS, and CdZnS/ZnS core/shell quantum dots: characterization and diffusion mechanism, Mater. Sci. Semicond. Process. 16 (2013) 1723–1729.
[11] M.A. Boles, M. Engel, D.V. Talapin, Self-assembly of colloidal nanocrystals: from intricate structures to functional materials, Chem. Rev. 116 (2016) 11220–11289.
[12] J. Hu¨hn, C. Carrillo-Carrion, M.G. Soliman, C. Pfeiffer, D. Valdeperez, A. Masood, I. Chakraborty, L. Zhu, M. Gallego, Z. Yue, M. Carril, N. Feliu, A. Escudero, A.M. Alkilany, B. Pelaz, P.D. Pino, W.J. Parak, Selected standard protocols for the synthesis, phase transfer, and characterization of inorganic colloidal nanoparticles, Chem. Mater 29 (2017), pp. 399–461.
[13] X. Zhong, M. Han, Z. Dong, T.J. White, W. Knoll, Composition-tunable $Zn_xCd_{1-x}Se$ nanocrystals with high luminescence and stability, J. Am. Chem. Soc. 125 (2003) 8589–8594.
[14] X. Zhong, Y. Feng, W. Knoll, M. Han, Alloyed $Zn_xCd_{1-x}S$ nanocrystals with highly narrow luminescence spectral width, J. Am. Chem. Soc. 125 (2003) 13559–13563.
[15] S.K. Panda, S.G. Hickey, C. Waurisch, A. Eychmüller, Gradated alloyed CdZnSe nanocrystals with high luminescence quantum yields and stability for optoelectronic and biological applications, J. Mater. Chem. 21 (2011) 11550–11555.
[16] D.W. Jeong, J.Y. Park, H.W. Seo, N.V. Myung, T.Y. Seong, B.S. Kim, One-pot synthesis of gradient interface quaternary ZnCdSSe quantum dots, Appl. Surf. Sci. 415 (2017) 19–23.
[17] Z. Yang, L. Lu, C.J. Kiely, B.W. Berger, S. McIntosh, Single enzyme direct biomineralization of CdSe and CdSe-CdS core-shell quantum dots, ACS Appl. Mater. Interfaces 9 (2017) 13430–13439.
[18] Y. Wang, K.S. Leck, V.D. Ta, R. Chen, V. Nalla, Y. Gao, T.C. He, H.V. Demir, H.D. Sun, Blue liquid lasers from solution of CdZnS/ZnS ternary alloy quantum dots with quasi-continuous pumping, Adv. Mater. 27 (2015) 169–175.
[19] W.K. Bae, L.A. Padilha, Y.S. Park, H. Mcdaniel, I. Robel, J.M. Pietryga, V.I. Klimov, Controlled alloying of the core/shell interface in CdSe/CdS quantum dots for suppression of auger recombination, ACS Nano 7 (2013) 3411–3419.
[20] X.B. Wang, W.W. Li, K. Sun, Stable efficient CdSe/CdS/ZnS core/multi-shell nanophosphors fabricated through a phosphine-free route for white light-emitting-diodes with high color rendering properties, J. Mater. Chem. 21 (2011) 8558–8565.
[21] D. Roy, T. Routh, A.V. Asaithambi, S. Mandal, P.K. Mandal, Spectral and temporal optical behavior of blue-, green-, orange-, and red-emitting CdSe-based core/gradient alloy shell/shell quantum dots: ensemble and single-particle investigation results, J. Phys. Chem. C 120 (2016) 3483–3491.
[22] Z.H. Chen, W.Q. Peng, K. Zhang, J. Zhang, M. Yanagida, L.Y. Han, Surface ion transfer growth of ternary $CdS_{1-x}Se_x$ quantum dots and their electron transport modulation, Nanoscale 4 (2012) 7690–7697.
[23] B.C. Fitzmorris, Y.C. Pu, J.K. Cooper, Y.F. Lin, Y.J. Hsu, Y. Li, J.Z. Zhang, Optical properties and exciton dynamics of alloyed core/shell/shell $Cd_{1-x}Zn_xSe/ZnSe/ZnS$ quantum dots, ACS Appl. Mater. Interfaces 5 (2013) 2893–2900.
[24] K. Boldt, N. Kirkwood, G.A. Beane, P. Mulvaney, Synthesis of highly luminescent and photo-stable, graded shell $CdSe/Cd_xZn_{1-x}S$ nanoparticles by in situ alloying, Chem. Mater. 25 (2013) 4731–4738.
[25] J. Owen, L. Brus, Chemical synthesis and luminescence applications of colloidal semiconductor quantum dots, J. Am. Chem. Soc. 139 (2017) 10939–10943.
[26] D.V. Talapin, I. Mekis, S. Götzinger, A. Kornowski, O. Benson, H. Weller, CdSe/CdS/ZnS and CdSe/ZnSe/ZnS core-shell-shell nanocrystals, J. Phys. Chem. B 108 (2004) 18826–18831.
[27] J. Cho, Y.K. Jung, J.K. Lee, H.S. Jung, Highly efficient blue-emitting CdSe-derived core/shell gradient alloy quantum dots with improved photoluminescent quantum yield and enhanced photostability, Langmuir 33 (2017) 3711–3719.
[28] Z. Győri, Z. Kónya, Á. Kukovecz, Synthesis and characterization of composition-gradient based $Cd_xZn_{1-x}Se_yS_{1-y}$ heterostructured quantum dots, React. Kinet. Mech. Catal. 115 (2015) 129–141.
[29] K.H. Lee, J.H. Lee, H.D. Kang, C.Y. Han, S.M. Bae, Y. Lee, J.Y. Hwang, H. Yang, Highly fluorescence-stable blue CdZnS/ZnS quantum dots against degradable environmental conditions, J. Alloy. Compd. 610 (2014) 511–516.
[30] P. Reiss, M. Protiere, L. Li, Core/shell semiconductor nanocrystals, Small 5 (2009) 154–168.
[31] K. Susumu, L.D. Field, E. Oh, M. Hunt, J.B. Delehanty, V. Palomo, P.E. Dawson, A.L. Huston, I.L. Medintz, Purple-, blue-, and green-emitting multishell alloyed quantum dots: synthesis, characterization, and application for ratiometric extracellular pH sensing, Chem. Mater. 29 (2017) 7330–7344.